COMMUNICATIONS IN COMPUTATIONAL PHYSICS
Vol. **5**, No. 2-4, pp. 635-648

Commun. Comput. Phys.
February 2009

Spectral Vanishing Viscosity Stabilized LES of the Ahmed Body Turbulent Wake

M. Minguez[1,2], R. Pasquetti[1,*] and E. Serre[2]

[1] *Lab. J.A. Dieudonné, UMR CNRS 6621, Université de Nice-Sophia Antipolis, 06200 Nice, France.*
[2] *Lab. MSNM-GP, UMR CNRS 6181, Université de Provence, 13451 Marseille, France.*

Received 26 September 2007; Accepted (in revised version) 31 March 2008

Available online 1 August 2008

Abstract. The paper addresses the Large-Eddy Simulation (LES) of the turbulent wake of the Ahmed car model. To this end we use a Fourier-Chebyshev multi-domain solver and the LES capability is implemented through the use of the Spectral Vanishing Viscosity (SVV) method, completed with a near-wall correction. A "pseudo-penalization" technique is used to model the bluff body. Comparisons of the present SVV-LES results with the experiments and also with a more classical Finite Volume LES are provided.

AMS subject classifications: 76D25, 76M22

Key words: Large-eddy simulation, spectral vanishing viscosity, spectral methods, wakes, turbulence.

1 Introduction

When computing turbulent flows, the computational grid is generally too coarse to capture the smaller scale phenomena, so that to prevent a numerical crash using a stabilization technique becomes necessary. This is especially true when high order methods are concerned, because the numerical scheme is then definitively not dissipative enough to stabilize the computation. This stabilization may result from a Sub Grid Scale (SGS) model, which aim is to provide an approximation of what happens at the "non-resolved scales", giving then rise to the usual Large-Eddy Simulation (LES) methodology (see, *e.g.*, [38]). Thus, the celebrated SGS Smagorinsky model completes the Navier-Stokes equations with an additional dissipation term, which diffusion coefficient is proportional to a norm of the strain rate tensor (symmetric part of the velocity gradient tensor).

*Corresponding author. *Email addresses:* `minguez@l3m.univ-mrs.fr` (M. Minguez), `richard.pasquetti@unice.fr` (R. Pasquetti), `eric.serre@l3m.univ-mrs.fr` (E. Serre)

The spectral vanishing viscosity (SVV) method was developed to handle hyperbolic 1D scalar problems, typically the Burgers equation, with standard Fourier or Legendre spectral methods [27,39]. The main goal was to provide stability together with preserving the so-called spectral accuracy, *i.e.*, the exponential rate of convergence of the numerical approximation. Basically, the method relies on the introduction of some artificial viscosity only in the high frequency range of the spectral approximation. This idea has appeared very useful in the frame of the LES of turbulent flows, resulting in the development of the so-called SVV-LES by extending to the incompressible Navier-Stokes equations ideas first developed for the Burgers equations [17,18].

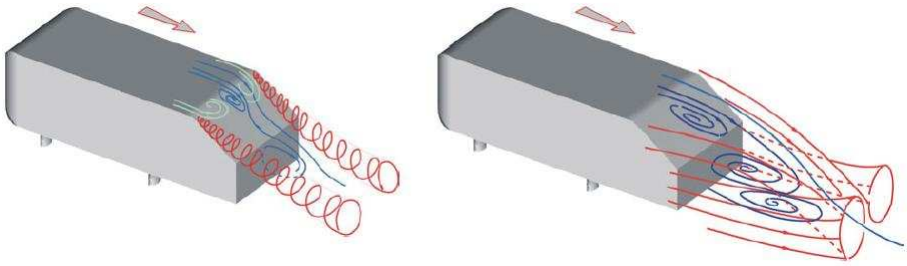

Figure 1: Car model and schematic of the flow for two slant angles (courtesy H. Lienhart): 25^o and 35^o (change of topology for 30^o).

Here we want to outline the efficiency of the SVV stabilization by addressing a challenging benchmark: the turbulent wake of the Ahmed car model [1]. As shown in the schematic of Fig. 1, the model is very crude, since essentially characterized by its length, height and width and by the length and inclination of the slant. However, for a Reynolds number, based on the height of the vehicle and on the incoming air velocity, equal to $Re=768000$, the flow is already very complex. Especially, depending on the slant inclination angle, the flow may show different topologies: For angles greater than a critical value of 30^o, then one observes a large detachment whereas for smaller angles there is a reattachment on the slant and the development of trailing vortices from its edges. Associated to this change in the flow topology, one observes a drag crisis, with a sudden decrease of the drag coefficient [1]. The Ahmed problem is presently not accessible to the Direct Numerical Simulation (DNS), *i.e.*, to the numerical integration of the Navier-Stokes equations, the Reynolds number being too high. Moreover, for the subcritical slant angle Reynolds Averaged Navier-Stokes (RANS) approaches fail to predict the correct behavior of the flow, see *e.g.* [13,28], and the LES methods must use a large amount of grid points to get valuable, but still far from fully satisfactory, results.

Another difficulty of this wake flow problem comes from the complexity of the geometry, much more complex than those accessible to standard spectral methods. This problem is addressed by using a volume penalization method, namely the *pseudo-penalization method* [35]. Here we revisit this approach, first for the paper to be self contained and second because the approximation of the obstacle is strongly linked to the treatment and

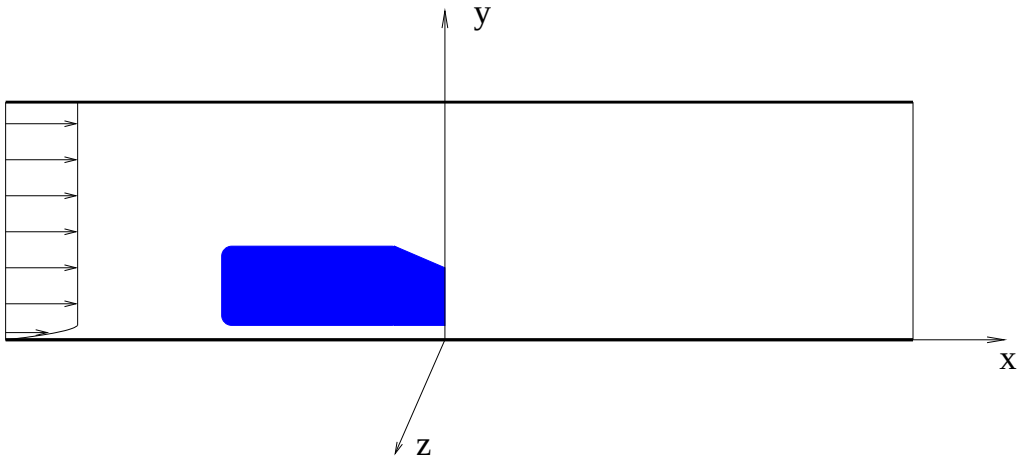

Figure 2: Schematic of the wake flow problem.

modeling of the boundary layers that form at the surface of the Ahmed body. Thus, just like a Near Wall (NW) model may be necessary in the frame of the LES, when the boundary layers are too thin to be resolved, it appears that adjustments of the pseudo-penalization and SVV approaches allow valuable improvements of the results.

The paper presents a state of the art of the SVV-LES approach that we are developing and points out that encouraging results may be obtained for a benchmark addressed for the first time with a high order method. It is organized as follows: Firstly we present the SVV-LES solver. To this end we start with the modeling, mention the main characteristics of the code, briefly describe the pseudo-penalization method and our implementation of the SVV technique for the Navier-Stokes equations and suggest a NW adjustment. Secondly we go into the details of our numerical results, with comparisons to the experimental data of [24] and to the LES results of [14]. Finally we conclude with some remarks.

2 The SVV-LES solver

2.1 Modeling

The flow is assumed to be governed by the incompressible Navier-Stokes (NS) equations. The computational domain is channel-like, see Fig. 2, and the horizontal z-direction is periodic.

All details concerning the exact geometry of the Ahmed car model may be found elsewhere, see, *e.g.*, [14]. Let us however recall that with H, L and W for its height, length and width, respectively, and S for the length of the slant, we have $H=288mm$, $L=3.625H$, $W=1.35H$ and $S=0.77H$. As usual for wake flow problems, the computational domain Ω must be much larger, especially its length. The aspect ratio is then large: The

computations have been carried out with $\Omega=[-2L,2L]\times[0,0.96L]\times[-0.65L,0.65L]$, the obstacle being located as shown in Fig. 2.

The Reynolds number equals $Re=UH/\nu=768000$, where U is the mean upstream velocity and ν the kinematic viscosity. The boundary conditions are the following: no-slip condition at the obstacle and at the ground, free-slip condition above the obstacle and boundary layer like profile at the inlet. Periodicity is assumed versus the z-direction. At the initial time the fluid is at rest.

2.2 The numerical solver

The main characteristics of the solver are the following:

- The approximation in space makes use of:
  - A Fourier Galerkin approximation in the homogeneous spanwise z-direction,
  - A domain decomposition in the elongated streamwise x-direction. A Schur complement method is used to compute, via direct solves of block tridiagonal systems, the subdomain interface values.
  - Chebyshev expansions in x and y (collocation method).
- A pseudo-penalization technique is used to model the bluff body [35]. Details on this approach are given in next Section.
- The time-scheme is globally second order accurate and makes use of 3 steps:
  - an explicit transport step. An Operator Integration Factor (OIF) semi-Lagrangian method is used to take into account the convective terms [9,26,41] and the transport equations which provide the values of the velocity components at the feet of the characteristics issued from the grid-points are solved with a fourth order Runge Kutta algorithm.
  - an implicit diffusion step. The time derivatives are approximated by using second order backward differences. The stabilizing SVV technique, used to go from the DNS to the LES version of the code, is implemented in this step.
  - a projection step. The velocity field obtained in the diffusion step is projected onto the space of the divergence free vector fields. To this end we use a unique grid "$\mathbb{P}_N-\mathbb{P}_{N-2}$" approximation [3]. However, the technique has been adapted to the case of our multidomain approach, *i.e.*, pressure values are computed at all the inner grid-points, including the domain interface points [8].
- Parallelization/vectorization: each subdomain is associated to one processor, which may be vectorial to still enhance the computational efficiency of the code.

2.3 The pseudo-penalization method

The standard volume penalization method consists in introducing in the NS equations a penalty term. With χ for the characteristic function of the obstacle and $C\gg 1$ a constant

coefficient, the penalized NS equations read:

$$D_t \boldsymbol{u} = -\nabla p + \nu \Delta \boldsymbol{u} - C\chi \boldsymbol{u} \tag{2.1}$$

with t for the time, $\boldsymbol{u}$ for the velocity, p for a pressure term and where D_t is the material derivative. Clearly, outside the obstacle we recover the NS equations, whereas inside the obstacle if C is infinite then $\boldsymbol{u}=0$. This approach has motivated a lot of numerical as well theoretical studies, see, *e.g.*, [2,20]. The main problem is that the penalty term may induce stability problem, if handled explicitly, or ill conditioned systems of equations, if handled implicitly.

To introduce the pseudo-penalization method, let us restart from the NS system (momentum and continuity equations) and assume that the linear diffusive term is treated implicitly, whereas the non-linear convective term is treated explicitly. Then the following semi-discrete equations must be solved at each time-step:

$$\nu \Delta \boldsymbol{u}^{n+1} - \frac{\alpha}{\tau} \boldsymbol{u}^{n+1} - \nabla p^{n+1} = \boldsymbol{f}^{n+1} \quad in\, \Omega, \tag{2.2}$$

$$\nabla \cdot \boldsymbol{u}^{n+1} = 0, \tag{2.3}$$

where n is the time index, τ the time-step and α a scheme dependent coefficient ($\alpha=3/2$ for a second-order backward finite difference scheme). The pair $(\boldsymbol{u}^n, p^n)$ is the numerical approximation of $(\boldsymbol{u}, p)$ at time t_n and $\boldsymbol{f}^{n+1}$ is an easily identifiable source term, which also depends on the time scheme.

With again χ for the characteristic function of the obstacle, the pseudo-penalization method consists then in solving:

$$\nu \Delta \boldsymbol{u}^{n+1} - \frac{\alpha}{\tau} \boldsymbol{u}^{n+1} - \nabla p^{n+1} = (1-\bar{\chi}) \boldsymbol{f}^{n+1} \quad in\, \Omega, \tag{2.4}$$

$$\nabla \cdot \boldsymbol{u}^{n+1} = 0, \tag{2.5}$$

where $\bar{\chi}$ is a regularized characteristic function, in practice obtained from local averages of the function χ. Clearly, inside the obstacle $(\boldsymbol{u}, p)$ solves now the Stokes equations with a $\mathcal{O}(1/\tau)$ penalization term. Details and full justification of this approach are provided in [35], where we explain that the regularization allows to better approximate the obstacle and to weaken the Gibbs phenomenon and also point out that it is then coherent to use a $\mathcal{O}(1/\tau)$, rather than "infinite", penalization coefficient. The expected results of this pseudo-penalization approach are the following:

- $|\boldsymbol{u}| = \mathcal{O}(\tau)$ inside the obstacle.
- A numerical boundary layer with $\mathcal{O}(h)$ thickness, where h is the local grid size.

Numerical results for a classical benchmark, the wake of a cylinder at Reynolds number $Re=200$, are provided in [35]. It appears that the Strouhal number (dimensionless frequency of the vortex shedding), the recirculation length and the minimal mean velocity in the recirculation bubble, as well as the time variations of the drag and lift coefficients are correctly computed.

2.4 LES and SVV stabilization

The standard LES methodology is based on the *filtered NS equations*, in which appears the *SGS tensor*. During the three last decades, various methods have been developed to model the SGS tensor: Smagorinsky, Scale similarity, Approximate Deconvolution Method (ADM), structure function, spectral viscosity (EDQNM theory), see *e.g.* [11,23,38] or [5] in the frame of spectral element methods.

More recently, some non-standard approaches have been proposed for LES. Basically, they make use of stabilization techniques. Among them one may discern:

• *Implicit LES (ILES)* approaches, which are based on non-linear schemes developed for hyperbolic equations. The main characteristic of such schemes is to supply artificial dissipation when required [4].

• *Variational Multi Scale (VMS)* formulations. The main idea is here to separate the low and high spatial frequencies and then to only model the smaller scales, see *e.g.* the earlier work [15].

• the SVV stabilization, as first proposed for LES in [17]. For us we began with a mixed ADM-SVV approach [30] before developing the SVV-LES [31–34, 42].

In the SVV-LES version of the solver we consider the following stabilized NS equations:

$$D_t\boldsymbol{u} = -\nabla p + \nu\nabla\cdot S_N(\nabla\boldsymbol{u}) \tag{2.6}$$

with S_N a diagonal operator which depends on the space discretization parameter N:

$$S_N \equiv diag\Big\{1+\frac{\epsilon_{N_i}}{\nu}Q^i_{N_i}\Big\}_{i=1,\cdots,3}, \tag{2.7}$$

where the subscript i denotes the i-direction (we use here x_i for x, y and z) and where appear the amplitude coefficient and spectral viscosity operator, ϵ_N and Q_N in 1D, as introduced in the periodic case (Fourier approximation) in [39] and in the non-periodic case (Legendre approximation) in [27].

Details on this formulation of the SVV method for the 3D NS equations may be found in [33, 42]. Let us recall that ϵ_N is usually a $\mathcal{O}(1/N)$ coefficient and the operator Q_N acts on the upper part of the Fourier, Legendre or Chebyshev spectrum of the spectral approximation: With *e.g.* φ_k for the Legendre polynomial of degree k, if $v=\sum_{k=0}^{\infty}\hat{v}_k\varphi_k$, then

$$Q_N(v) = \sum_{k=0}^{N}\hat{Q}_k\hat{v}_k\varphi_k,$$

with $1\geq\hat{Q}_k>0$ if $k>m_N$ and $\hat{Q}_k=0$ if $k\leq m_N$. In practice we use the formula introduced in [27],

$$\hat{Q}_k = \exp(-(k-N)^2/(k-m_N)^2) \quad \text{if } k>m_N.$$

For the Ahmed body problem we use mappings in the x-streamwise and y-crossflow directions. Since the polynomial approximation holds in the reference domain, say $\hat{\Omega}$,

with the mapping $\boldsymbol{f}:\hat{\Omega}\to\Omega$, the operator S_N is defined as follows:

$$S_N(\nabla\boldsymbol{u})\equiv S_N(\hat{\nabla}\hat{\boldsymbol{u}})\,G, \tag{2.8}$$

where G is the Jacobian matrix of $\boldsymbol{f}^{-1}$ and $\hat{\boldsymbol{u}}=\boldsymbol{u}\circ\boldsymbol{f}$.

The practical implementation of the operator S_N is based on the introduction of SVV modified differentiation matrices. From the previous definition of S_N we indeed have:

$$[\nabla\cdot S_N(\nabla\boldsymbol{u})]_i=\sum_j\partial_j(\tilde{\partial}_j\boldsymbol{u}_i), \tag{2.9}$$

where $\tilde{\partial}_j=(1+\nu^{-1}\epsilon_{N_j}Q^j_{N_j})\partial_j$.

2.5 Near wall correction

For very high Reynolds number flows, the boundary layers at the walls become very thin and the mesh is then too coarse to allow a correct calculation. One must then associate to the LES a NW model [37]. This field is very active but often developed for Finite Volume approximations. In the frame of the present spectral approximation and when using a penalization type method, inserting such NW models remains an open problem.

As expected, for the Ahmed body computation our first numerical experiments have shown that the boundary layers were not resolved and that the turbulence intensity was there too low. Typically, for $Re=768000$ the distance from the first grid-point to the wall is $\mathcal{O}(100)$ viscous wall units, which is too much important to resolve the boundary layer. It was thus suitable to introduce some NW correction.

Our numerical experiments have shown that the results could be significantly improved if:

• The bluff body characteristic function was not regularized;

• The SVV dissipation was decreased in the NW region, by changing the SVV parameters at the first grid-points (1 or 2 points) close to the walls. A similar idea was also suggested in [18], where the so-called Panton function [29] was used to smoothly cancel the SVV term at the walls.

This may be formulated as:

$$D_t\boldsymbol{u}=-\nabla p+\nu\nabla\cdot S_N(\nabla\boldsymbol{u})-C\chi\boldsymbol{u}+\boldsymbol{f}_{BL} \tag{2.10}$$

with BL for Boundary Layer and where:

$$\boldsymbol{f}_{BL}=\chi_{BL}\nu\nabla\cdot(S^{BL}_N(\nabla\boldsymbol{u})-S_N(\nabla\boldsymbol{u})). \tag{2.11}$$

In this expression χ_{BL} is a second characteristic function used to localize the NW adjustment, whereas the non-regularized function χ is used to model the bluff body via the pseudo-penalization technique. The operator S^{BL}_N is defined like S_N but makes use of a smaller value of ϵ_N and / or a greater value of m_N.

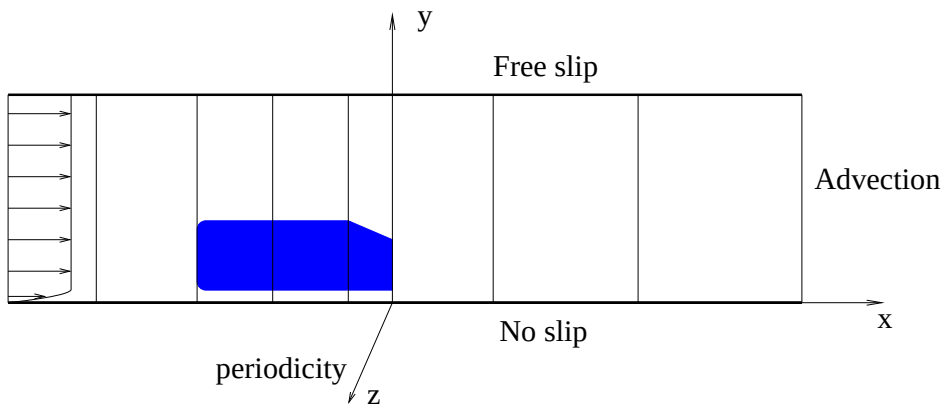

Figure 3: Schematic of the domain decomposition and boundary conditions.

Basically the idea is to decrease the SVV dissipation in the NW region. However, in the frame of a spectral approximation it is probably more relevant to simply view the source term f_{BL} as a boundary layer destabilizing term, allowing the expected increase of the turbulence intensity in the NW regions. Such a term can be easily taken into account if treated explicitly. To this end we simply use a second order Adams-Bashforth extrapolation at the resolution time, t_{n+1}, consistent with the global accuracy of the scheme. Note that this explicit treatment has never induced extra numerical stability constraint, certainly because the term f_{BL} is very localized.

3 Numerical results

The multi-domain decomposition is shown in Fig. 3. We use 8 subdomains and in each of them the polynomial approximation degrees in streamwise and crossflow directions are $N_x=40$ and $N_y=190$, respectively. In the z-spanwise direction we use $2N_z=340$ grid-points. This multi-domain discretization yields approximately 21.3×10^6 grid-points. In order to fit at best the Ahmed body, subdomain interfaces have been located at the front and rear parts and also at the beginning of the slant. In order to accumulate grid-points at the roof, a non-linear mapping is used in the y direction. In the z-direction, which is handled with Fast Fourier Transform, we simply increase the number of grid-points, knowing that the computational cost growth is only weakly superlinear with respect to N_z. The resulting mesh is of course not optimal, but it allows the use of very efficient solvers and so a large number of grid-points. However, the present mesh is not relevant for a DNS, since the grid step is only of the order of the Taylor microscale and the NW regions are not resolved, the first NW grid-points being at 100 to 400 wall units from the Ahmed body. The LES approach and the NW treatment are thus fully justified.

In each direction the following SVV control parameters are used: $m_N=\sqrt{N}, \epsilon_N=1/N$. In the NW region we have only changed the SVV activation parameter m_N, in an anisotropic way: $m_N=\{2\sqrt{N_x},5\sqrt{N_y},4\sqrt{N_z}\}$, at the two first grid-points the nearest of

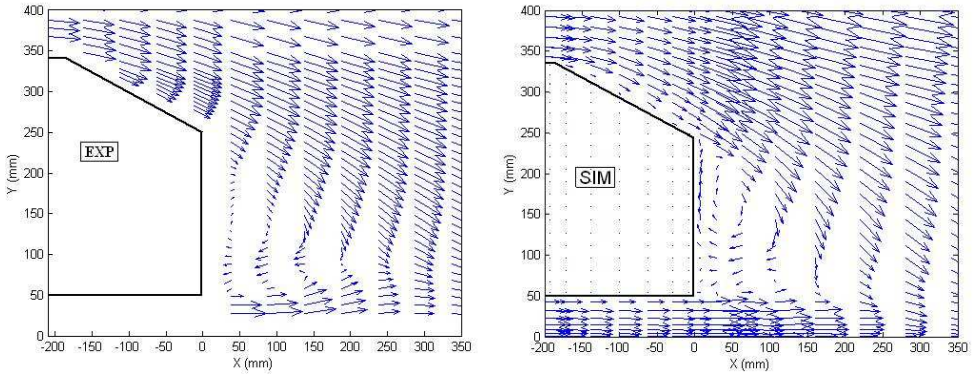

Figure 4: Experimental (left) and simulated (right) mean velocity in the vertical median plane.

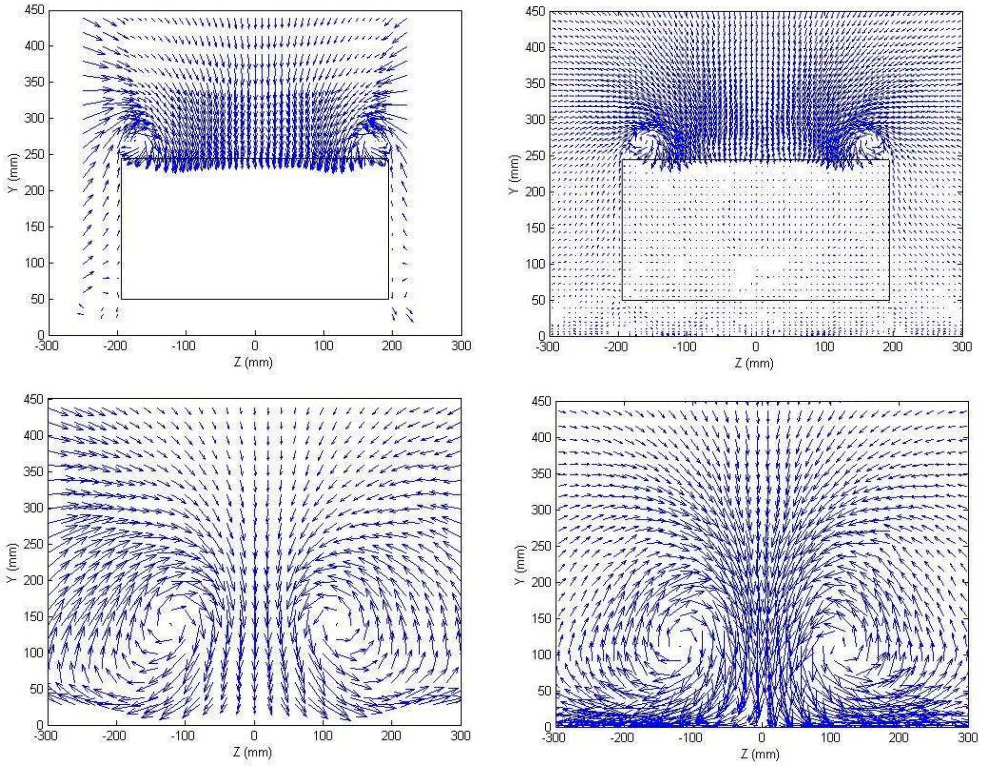

Figure 5: Experimental (left) and simulated (right) mean velocity fields in the planes $x=0mm$ (top) and $x=500mm$ (bottom).

the obstacle walls (NW correction). The time-step equals 2×10^{-3} and 40 time units, H/U, are used to compute the statistics. This time interval is certainly too short to obtain fully converged statistics but appears large enough to obtain valuable results, *e.g.*, showing a satisfactory symmetry with respect to the median plane $z=0$.

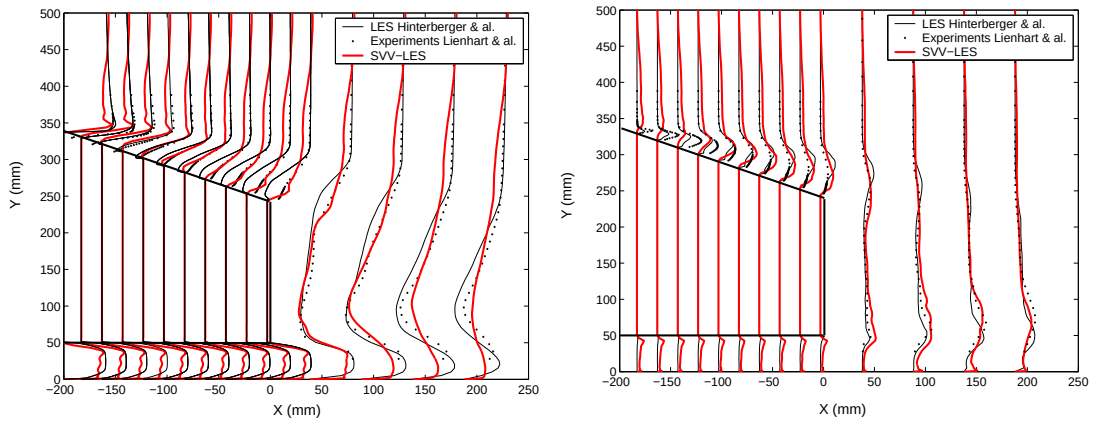

Figure 6: Mean streamwise velocity (left) and turbulent kinetic energy profiles (right). Comparisons with the LES of Hinterberger *et al.* (2004) and with the experiment of Lienhart *et al.* (2000).

Qualitatively the simulated flow agrees with the experiments. Especially, the reattachment on the slant and the trailing vortices which escape from the slant edges are observed. More quantitatively one can first compare some relevant mean velocity fields with the experimental data obtained in [24]. Fig. 4 presents mean velocity fields in the median vertical plane $z=0$, around the rear part of the obstacle. Similar comparisons are done in the planes $x=0mm$ and $x=500mm$ in Fig. 5. The agreement between the numerical and experimental results appears satisfactory. Beyond the similarities of the computed and measured vector fields, one can observe that the recirculation length is well predicted and that the trailing vortices issued from the slant edges are well recovered.

Mean streamwise velocity and turbulent kinetic energy profiles at different x-stations on the slant are shown in Fig. 6. Our SVV-LES results are here again compared with the experimental data of [24] but also with LES results [14]. The LES has been carried out with the parallelized version of the code LESOCC (Large Eddy Simulation On Curvilinear Coordinate) [6]: (i) the space approximation makes use of central second order finite difference approximations for both the convective and diffusive terms, (ii) time advancement is explicit (Runge-Kutta method) and (iii) conservation of mass is achieved with the SIMPLE algorithm, see, *e.g.*, [36]. The LES capability is implemented with the standard Smagorinsky model together with a Werner-Wengle [40] type NW model, but assuming an instantaneous logarithmic profile rather than a power law profile. Note here that the efficiency of the LESOCC solver essentially results from using an explicit time scheme, which is not suitable for stability reasons when spectral approximations are concerned, whereas thanks to the penalization technique, the geometry is in our case Cartesian. Similar problems, in terms of number of degrees of freedom, may then be faced by the LES [14] and present SVV-LES solvers.

The mean streamwise velocity profiles, see Fig. 6 (left), are not fully satisfactory: The general trend is captured but discrepancies with the experimental data may be ob-

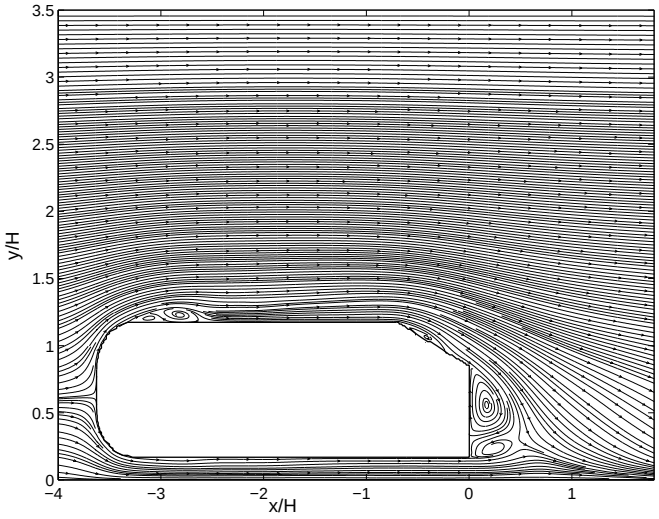

Figure 7: Mean two-dimensional streamlines in the plane $z=0$.

served. Especially, one has a deficit of the SVV-LES profiles in the upper part of the flow ($350mm < y < 450mm$). The LES [14] shows a better agreement with the measurements in this region and at the beginning of the slant, whereas the present SVV-LES results are in better agreement with the experimental data from mid-slant. The profiles of turbulent kinetic energy are shown in Fig. 6 (right). Here again the general trend is captured but improvements are still required. As could be expected, one observes an overestimation of the turbulent kinetic energy in the upper part of the flow which corresponds to the velocity profile deficit previously mentioned. Despite not completely satisfactory, such profiles are much better than those obtained with a coarser mesh (4.68×10^6 grid-points) or without NW correction.

A more detailed analysis shows that this deficit of streamwise velocity coupled to an excess of turbulent kinetic energy is confined in the median region, say for $-150mm < z < 150mm$. Moreover, the phenomenon develops from the front part of the body, downstream of a recirculation bubble localized at $x/H \approx -3$, see Fig. 7. Similar recirculation bubbles are obtained on the lateral sides. Such a recirculation bubble is not obtained in [14] and it is not known if it was observed in the experiments [24]. At this point the discussion joins the one developed in [21, 22], where the Ahmed body flow at the lower Reynolds number $Re = 200000$ is addressed. The authors report the occurrence of a recirculation bubble on the roof, as well as similar ones of the lateral sides, discuss the importance of these recirculation zones on the downstream development of the flow, but cannot conclude if at the higher Reynolds number $Re=768000$ such recirculation bubbles are still present. Our SVV-LES computation of the Ahmed body flow may correspond to an effective Reynolds number lower than the one of the experiments, as can be feared from non-resolving properly the boundary layers and as it is generally the case in under-resolved LES, but additional experimental results would be welcome.

4 Concluding remarks

Valuable SVV-LES results for a difficult problem have been obtained: RANS approaches fail and up to now no LES results are fully satisfactory for the Ahmed flow, especially for a slant angle equal to 25^o. A high number of grid-points is required: Our first coarse grid computations (4.68×10^6 grid-points) failed to predict the turbulence intensity. However, improvements are still needed to obtain fully satisfactory results.

The present LES approach is based on the SVV stabilization technique (SVV-LES approach). With respect to VMS-LES methods, the artificial viscosity is smoothly integrated in the high frequency range. With respect to the well known Chollet-Lesieur spectral viscosity [7], based on the Eddy Damped Quasi Normal Markovian (EDQNM) theory, the artificial viscosity is only integrated in the high frequency range. Our 3D SVV formulation is based on a matrix form of the SVV operator involving 1D viscosity operators. This differs *e.g.* from the earlier work [17] or more recently from [19]. Alternative strategies may also be found in [10, 16]. Variants in the SVV stabilization are proposed in [12, 25]. In our formulation and implementation of the SVV stabilization, there is no additional computational cost of the SVV-LES with respect to DNS. This results from the fact that the SVV modified differentiation matrices are set up in a preliminary calculation. Thus the algorithm is not changed during the time integration. To get valuable statistics the computational time remains important, typically $400h$ on a NEC SX8 parallel-vectorial computer.

Some difficult problems remain: the NW correction presently used is certainly not sufficient to recover a reliable description of the turbulent boundary layer dynamics, since the sub-cell dynamics includes turbulence kinetic energy production, a phenomenon which cannot be taken into account by just reducing the subgrid dissipation. It would be suitable to use a relevant NW model, in conjunction with the use of our penalty type technique. NW models have been essentially developed in the frame of Finite Volume approximations. It should also be mentioned that the drag coefficient that we presently obtain is overestimated.

Acknowledgments

The computations were done on the NEC-SX8 Computer of the IDRIS Computational Center (project 064055) and on the parallel computer of the SIGAMM Computational center at the OCA (Nice). The work was supported by the CNRS in the frame of the DFG-CNRS program "LES of complex flows".

References

[1] S.R. Ahmed and G. Ramm, Some salient features of the time-averaged ground vehicle wake, SAE Technical Paper 840300 (1984).

[2] P. Angot, C.H. Bruneau and P. Fabrie, A penalization method to take into account obstacles in incompressible viscous flows, Numerische Mathematik, 81 (1999), 497-520.
[3] M. Azaiez, A. Fikri and G. Labrosse, A unique grid spectral solver of the nD Cartesian unsteady Stokes system. Illustrative numerical results, Finite Elem. Anal. Des., 16 (3-4) (1994), 247-260.
[4] J.P. Boris, F.F. Grinstein, E.S. Oran and R.L. Kolbe, New insights into large eddy simulation, Fluid Dyn. Res., 10 (1992), 199-228.
[5] R. Bouffanais, M.O. Deville and E. Leriche, Large-Eddy Simulation of the flow in a lid-driven cubical cavity, Phys. Fluids, 19 (2007), Art. 055108.
[6] M. Breuer and W. Rodi, Large eddy simulation of complex turbulent flows of practical interest, Notes on Numerical Fluid Mechanics, 52, E.H. Hirschel Ed., Vieweg, Braunschweig (1996), 258-274.
[7] J.P Chollet and M. Lesieur, Parametrization of small scales of three dimensional isotropic turbulence utilizing spectral closures, J. Atmos. Sci., 38 (1981), 2747-2757.
[8] L. Cousin and R. Pasquetti, High-order methods for the simulation of transitional to turbulent wakes, Advances in Scientific Computing and Applications, Y. Lu, W. Sun and T. Tang Eds, Science Press Beijing/New York (2004), 133-143.
[9] M.O. Deville, P.F. Fischer and E.H. Mund, High-Order Methods for Incompressible Flows, Cambridge University Press, 2002.
[10] G.Q. Chen, Q. Du and E. Tadmor, Spectral viscosity approximations to multidimensional scalar conservations laws, Math. Comput., 204 (1993), 629-643.
[11] B.J. Geurts, Elements of Direct and Large-Eddy Simulation, Cambridge University Press, 2004.
[12] B. Guo, H. Ma and E. Tadmor, Spectral vanishing viscosity method for nonlinear conservation laws, SIAM J. Numer. Anal., 39 (4) (2001), 1254-1268.
[13] E. Guilmineau, Computational study of flow around a simplified car body, J. Wind Eng. Ind. Aerodyn., in press (2007).
[14] M. Hinterberger, M. Garcia-Villalba and W. Rodi, Large eddy simulation of flow around the Ahmed body, in Lectures Notes in Applied and Computational Mechanics / The aerodynamic of heavy vehicles: Trucks, Buses and Trains, R. Mc Callen, F. Browand, J. Ross (Eds), Springer Verlag, ISBN: 3-540-22088-7, 2004.
[15] T.J.R. Hughes, L. Mazzei and A.A. Oberai, The multiscale formulation of large eddy simulation: Decay of homogeneous isotropic turbulence, Phys. Fluids, 13 (2) (2001), 505-512.
[16] O.S.M. Kaber, A Legendre pseudo-spectral viscosity method, J. Comput. Phys., 128(1) (1996), 165-180.
[17] G.S. Karamanos and G.E. Karniadakis, A spectral vanishing viscosity method for large-eddy simulation, J. Comput. Phys., 163, (2000), 22-50.
[18] R.M. Kirby and G.E. Karniadakis, Coarse resolution turbulence simulations with spectral vanishing viscosity - Large Eddy Simulation (SVV-LES) , J. Fluids Engineering, 124 (4) (2002), 886-891.
[19] R.M. Kirby and S.J. Sherwin, Stabilisation of spectral / hp element methods through spectral vanishing viscosity: Application to fluid mechanics modelling, Comput. Methods Appl. Mech. Engrg., 195 (2006), 3128-3144.
[20] K. Khadra, P. Angot, S. Parneix and J.P. Caltagirone, Fictitious domain approach for numerical modelling of Navier-Stokes equations, Int. J. Numer. Meth. Fluids, 34 (2000), 651-684.
[21] S. Krajnovic and L. Davidson, Large-eddy simulation of the flow around simplified car model, 2004 SAE Congress, SAE Paper No. 2004-01-0227, Détroit (USA).

[22] S. Krajnovic and L. Davidson, Large-eddy simulation of the flow around an Ahmed body, 2004 ASME HTFED04 Congress, Paper HT-FED2004-56325, Charlotte (USA).
[23] M. Lesieur, O. Métais, P. Comte, Large-Eddy Simulations of Turbulence, Cambridge University Press, 2004.
[24] H. Lienhart, C. Stoots and S. Becker, Flow and turbulence structures in the wake of a simplified car model (Ahmed body). DGLR Fach Symp. der AG STAB (2000).
[25] H.P. Ma, Chebyshev-Legendre superspectral viscosity method for non linear conservation laws, SIAM J. Numer. Anal., 35 (3) (1998), 893-908.
[26] Y. Maday, A.T. Patera and E.M. Ronquist, An operator-integration-factor splitting method for time-dependent problems: application to incompressible fluid flow, J. Sci. Comput., 5 (4) (1990), 263-292.
[27] Y. Maday, S.M.O. Kaber and E. Tadmor, Legendre pseudo-spectral viscosity method for nonlinear conservation laws, SIAM J. Numer. Anal., 30 (2) (1993), 321-342.
[28] R. Manceau and J.-P. Bonnet, "10th joint ERCOFTAC (SIG-15)/IAHR/QNET-CFD Workshop on Refined Turbulence Modelling", Poitiers, 2000.
[29] R.L. Panton, A Reynolds stress function for wall layers, ASME, J. Fluids Eng., 119 (1997), 325-330.
[30] R. Pasquetti and C.J. Xu, High-order algorithms for large eddy simulation of incompressible flows, J. Sci. Comp. , 17 (1-4) (2002), 273-284.
[31] R. Pasquetti, High-order LES modeling of turbulent incompressible flows, C.R. Acad. Sci. Paris, 333 (2005), 39-49.
[32] R. Pasquetti, Spectral vanishing viscosity method for LES: Sensitivity to the SVV control parameters, J. of Turbulence, 6, N12 (2005), Special issue: Marseille Euromech Colloquium 2004.
[33] R. Pasquetti, Spectral vanishing viscosity method for large eddy simulation of turbulent flows, J. Sci. Comp.. 27 (1-3) (2006), 365-375,
[34] R. Pasquetti, Spectral vanishing viscosity method for high-order LES: Computation of the dissipation rates, ECCOMAS CFD 2006 Congress (proceedings on line), Egmond aan Zee (Holland).
[35] R. Pasquetti, R. Bwemba and L. Cousin, A pseudo-penalization method for high Reynolds number unsteady flows, Appl. Numer. Math., to appear.
[36] S.V. Patankar, Numerical Heat Transfer and Fluid Flows, Series in Computational methods and thermal sciences, Hemisphere Publishing Corporation, 1980.
[37] U. Piomelli and E. Balaras, Wall-layer models for large-eddy simulations, Annu. Rev. Fluid Mech., 34 (2002), 349-374.
[38] P. Sagaut, Large-Eddy Simulation for Incompressible Flows: An Introduction, Series: Scientific Computation, Springer, 2005.
[39] E. Tadmor, Convergence of spectral methods for nonlinear conservation laws, SIAM J. Numer. Anal., 26 (1) (1989), 30-44.
[40] H. Werner and H. Wengle, Large-eddy simulation of turbulent flow over and around a cube in a plate channel, 8th Symp. on Turb. Shear Flows, Munchen, 1991.
[41] C.J. Xu and R. Pasquetti, On the efficiency of semi-implicit and semi-Lagrangian spectral methods for the calculation of incompressible flows, Inter. J. Numer. Meth. Fluids, 35 (2001), 319-340.
[42] C.J. Xu and R. Pasquetti, Stabilized spectral element computations of high Reynolds number incompressible flows, J. Comput. Phys., 196 (2) (2004), 680-704.